

NASA Technical Memorandum 107362

# Development of an Aeroelastic Code Based on an Euler/Navier-Stokes Aerodynamic Solver

Milind A. Bakhle, Rakesh Srivastava, and Theo G. Keith, Jr.

*University of Toledo*

*Toledo, Ohio*

George L. Stefko

*Lewis Research Center*

*Cleveland, Ohio*

J. Mark Janus

*Mississippi State University*

*Mississippi State, Mississippi*

November 1996



National Aeronautics and  
Space Administration



# **DEVELOPMENT OF AN AEROELASTIC CODE BASED ON AN EULER / NAVIER-STOKES AERODYNAMIC SOLVER**

**Milind A. Bakhle, Rakesh Srivastava, and Theo G. Keith, Jr.**  
University of Toledo  
Toledo, Ohio

**George L. Stefko**  
NASA Lewis Research Center  
Cleveland, Ohio

**J. Mark Janus**  
Mississippi State University  
Mississippi State, Mississippi

## **ABSTRACT**

This paper describes the development of an aeroelastic code (TURBO-AE) based on an Euler / Navier-Stokes unsteady aerodynamic analysis. A brief review of the relevant research in the area of propulsion aeroelasticity is presented. The paper briefly describes the original Euler / Navier-Stokes code (TURBO) and then details the development of the aeroelastic extensions. The aeroelastic formulation is described. The modeling of the dynamics of the blade using a modal approach is detailed, along with the grid deformation approach used to model the elastic deformation of the blade. The work-per-cycle approach used to evaluate aeroelastic stability is described. Representative results used to verify the code are presented. The paper concludes with an evaluation of the development thus far, and some plans for further development and validation of the TURBO-AE code.

## **INTRODUCTION**

NASA's Advanced Subsonic Technology (AST) program seeks to develop technologies to increase the fuel efficiency of commercial aircraft engines, improve the safety of engine operation, reduce the emissions, and reduce engine noise. With the development of new designs of ducted fans, compressors, and turbines to achieve these goals, a basic aeromechanical requirement is that there should be no flutter or high resonant blade stresses in the operating regime. In order to verify the aeroelastic soundness of the design, an accurate prediction of the unsteady

aerodynamics and structural dynamics of the propulsion component is required. The complex geometry, the possibility of shock waves and flow separation makes the modeling of the unsteady aerodynamics a difficult task. The advanced blade geometry, new blade materials and new blade attachment concepts, make the modeling of the structural dynamics a difficult problem.

Computational aeroelastic modeling of fans, compressors, and turbines, requires several simplifying assumptions. Flutter calculations are typically carried out assuming that the blade row is isolated. This simplifies the structural dynamics formulation and the unsteady aerodynamic calculations considerably.

For an isolated blade row flutter calculation, the modeling of the unsteady aerodynamics is the biggest challenge. Many simplifying assumptions are made in the modeling of the unsteady aerodynamics. In the past, a panel method based on linear compressible small-disturbance potential theory has been used to model the unsteady aerodynamics and aeroelasticity of propfans in subsonic flow [Williams, 1990, and Kaza et al., 1989]. The major limitation of this analysis is the neglect of transonic and viscous flow effects in the model. Although this analysis requires a fairly small computational effort, the inherent limitation in the model precludes its use in a majority of practical applications.

More recently, a full potential unsteady aerodynamic analysis has been used with a modal structural dynamics approach to model the aeroelastic behavior of fan blades [Bakhle and Reddy, 1993 and Bakhle et al., 1993]. In this aeroelastic analysis, the unsteady aerodynamics model is in the time domain. The time domain flutter calculations use the method of simultaneous integration of structural dynamics and aerodynamics equations in time. Alternatively, for the frequency domain flutter calculations, a Fourier analysis is required to transform the time domain unsteady aerodynamic force coefficients to the frequency domain. The eigenvalue approach is then used. Although the full potential aerodynamic formulation is able to model transonic effects to a certain extent (limited to weak shocks), the vortical effects are still neglected. Thus, for example, the blade tip vortex, or a leading-edge vortex is not modeled. Significant computational effort is required for such flutter calculations based on full potential aerodynamics. An aeroelastic analysis based on the Euler equations [Srivastava and Reddy, 1995] can model vortical flows, but viscous effects are not taken into account. Recently, other researchers [Hall, 1992, He and Denton, 1993, Gerolymos and Vallet, 1994, Peitsch et al., 1994, and Carstens, 1994] have also developed inviscid and viscous unsteady aerodynamic analyses for vibrating blades.

For aeroelastic problems in which viscous effects play an important role (such as flutter with flow separation, or stall flutter, and flutter in the presence of shock and boundary-layer interaction), a more advanced aeroelastic computational capability is required. This paper describes the development of such an aeroelastic code (TURBO-AE). This aeroelastic code is based on an unsteady aerodynamic Euler / Navier-Stokes code (TURBO), developed separately, which is described in the following section. In this paper, the grid deformation method is described, along with the interpolation from the finite-element structural mesh to the CFD mesh, and the calculation of the aeroelastic forces and work.

## DESCRIPTION OF EULER / NAVIER-STOKES CODE- TURBO

This section describes *very briefly* the TURBO code. Additional details regarding the code are available elsewhere [Janus, 1989 and Chen, 1991]. The TURBO code provides all the unsteady aerodynamics to the TURBO-AE code.

The TURBO code was originally developed [Janus, 1989] as an inviscid flow solver for modeling the flow through multistage turbomachinery. It has the capability to handle multiple blade rows with even or uneven blade count, stationary or rotating blade rows and blade rows at an angle of attack. Multiple blade passages are included in the calculation, when required. Additional developments were made [Chen, 1991] to incorporate viscous terms into the model. The code can now be applied to model realistic turbomachinery configurations with flow phenomena such as shocks, vortices, separated flow, secondary flows, and shock and boundary layer interactions.

The code is based on a finite volume scheme. Flux vector splitting is used to evaluate the flux Jacobians on the left hand side of the governing equations [Janus, 1989] and Roe's flux difference splitting is used to form a higher-order TVD (Total Variation Diminishing) scheme to evaluate the fluxes on the right hand side. Newton sub-iterations are used at each time step to maintain higher accuracy. A Baldwin-Lomax algebraic turbulence model is used in the code.

## DEVELOPMENT OF AEROELASTIC CODE - TURBO-AE

The TURBO-AE code assumes a normal mode representation of the structural dynamics of the blade. Thus, the dynamic characteristics of each blade are assumed to be represented in terms of in-vacuum modes, with the associated natural

frequency and generalized mass for each mode. Typically, a finite-element analysis code such as NASTRAN is used to calculate the modal data mentioned. No restriction is placed on the analysis, except that it should provide grid point coordinates, modal deflections, natural frequencies, and generalized mass for each mode of interest.

At the current stage of development, the aeroelastic code (TURBO-AE) models only in-phase blade vibrations. That is, the interblade phase angle is restricted to be zero. This is a limitation of the aeroelastic code and not of the original unsteady aerodynamics code (TURBO). Thus, in TURBO-AE, only one blade and one blade passage are modeled.

A work-per-cycle approach is used to determine aeroelastic (flutter) stability. Using this approach, the motion of the blade is prescribed to be a harmonic vibration in a specified in-vacuum normal mode with a specified frequency. The vibration frequency is typically the natural frequency for the mode of interest, but some other frequency can also be used. The aerodynamic forces acting on the vibrating blade and the work done by these forces on the vibrating blade during a cycle of vibration are calculated. If work is being done on the blade by the aerodynamic forces, the blade is dynamically unstable, since it will result in extraction of energy from the flow, leading to an increase in amplitude of oscillation of the blade. Note that coupled mode flutter cannot be modeled with this approach.

In the following two sub-sections, the grid deformation scheme and the work-per-cycle and generalized force calculations are detailed.

## **Grid Deformation**

The blade of a rotor undergoes a rigid-body rotation about the axis of the rotor and a simultaneous elastic deformation. This is modeled through grid point motion. This requires the calculation of a new grid at each time step. The grid point motion due to blade rotation consists simply of a rotation of each grid point about the axis of the rotor. There is no relative motion between grid points. The grid point motion due to the elastic deformation of the blade is superposed on this rotation. The elastic deformation of the blade does cause relative motion between grid points and therefore, the term grid deformation is used in this context.

The grid deformation approach [Huff, 1989] used in the TURBO-AE code is described here. In this approach, the grid points on the surface of the blade move by

an amount equal to the deformation of the blade. The grid points on the remaining boundaries of the computational domain do not move. The motion of the grid points in the interior of the computational domain is determined as a product of three coefficients (one for each computational coordinate direction) and the motion of points on blade surfaces. The coefficient in each computational direction is linearly dependent on the distances of the interior grid point from the boundaries and from the blade surfaces along that computational direction. Thus, points close to the moving blade move almost as much as points on the blade, and points close to the stationary boundaries do not move much at all. The coefficients are not presented here, but can be found in [Huff, 1989], where they are referred to as weighting functions.

The grid deformation is calculated as described here. First, new locations of all grid points on the blade surface are calculated. For a harmonic vibration of the blade in a selected in-vacuum normal mode, the displacement of any point on the blade (due to elastic deformation)  $\vec{X}(x,y,z,t)$  can be written in terms of the generalized coordinate  $q(t)$  and the modal deflection or mode shape function  $\vec{\delta}(x,y,z,t)$  as:

$$\vec{X}(x,y,z,t) = q(t) \vec{\delta}(x,y,z,t) \quad (1)$$

Note that  $x$ ,  $y$ , and  $z$  represent the coordinates in a rotating coordinate system. Further note that the modal deflection or mode shape function  $\vec{\delta}$  has been interpolated from the finite-element grid to the CFD grid. This interpolation, which is described in the following paragraph, is performed only once for each mode of interest.

The interpolation of the modal deflections from the finite element grid onto the CFD grid is accomplished as follows. The interpolation is done with the blade undeflected in a reference position. At each CFD grid point on the blade surface, the distance to the nearest three finite-element grid points is calculated. Then, the modal deflections at these three nearest neighbors are used in a bi-linear interpolation scheme to calculate the interpolated value of the modal deflection at that CFD grid point. The interpolated modal deflections  $\vec{\delta}$  are stored and used at each time step to calculate the motion of each grid point on the blade surface.

Next, the new locations of the interior points are calculated. This requires the calculation of coefficients based on the reference location of the interior grid point. As previously mentioned, the distance of each interior grid point, from the computational boundaries and from the blade surfaces, along the corresponding computational direction, is calculated. For example, for an interior grid point  $(i,j,k)$ ,

the distance to the nearest  $i = \text{constant}$  (inlet/exit) boundary is calculated along the  $i$ -direction coordinate line. Then, the distance from the interior point to the relevant blade surface ( $i$ -index corresponding to leading/trailing edge) is calculated along the  $i$ -direction coordinate line. These two calculations are repeated for the other two computational directions. Then, these distances are used to calculate the coefficients in the three computational coordinate directions. The motion of the interior grid points is simply a linear scaling of the motion of the blade surface.

Special attention is required for grid points located between the blade tip and the duct or casing. Typically, the grid points in this region are very closely spaced in the radial direction. If it is assumed that the grid points on the casing do not move when the blade deforms, the computational cells can become excessively skewed due to the motion of the blade tip and the interior grid points. To avoid this, the grid points on the casing are allowed to move (along the casing surface) in such a way as to reduce the skewing of the interior computational cells. The location of the grid points in the interior region is calculated by linear interpolation between the blade tip and the casing. This treatment improves the aspect ratio of the computational cells considerably.

### **Work and Force Calculation**

To determine aeroelastic stability using the work-per-cycle approach, the blade motion is specified to be harmonic:

$$q(t) = q_0 \sin(\omega t) \quad (2)$$

where  $q_0$  is the amplitude of motion and  $\omega$  is the vibration frequency.

The work-per-cycle done on the blade is calculated as:

$$W = \oint \int_S p \, d\vec{A} \cdot (\partial \vec{X} / \partial t) dt \quad (3)$$

or,

$$W = \oint \int_S p \, d\vec{A} \cdot \vec{\delta} q_0 \omega \cos(\omega t) dt \quad (4)$$



In the above,  $p = p(x, y, z, t)$  is the unsteady pressure on the blade surface due to blade vibration,  $\vec{A}$  is the blade surface area vector pointing *into* the blade surface,  $\int_S$  is the integral over the blade surface,  $\oint$  is the integral over one cycle of blade vibration. For viscous calculations, the viscous stresses must be included in the calculation along with the pressure. This is done in the TURBO-AE code, but the expressions for the work including inviscid and viscous contributions are not presented here.

The work-per-cycle is an indicator of aeroelastic stability. The blade is dynamically unstable if the work done on the blade during a cycle of blade vibration is positive.

Finally, the generalized force on the blade  $A_{m,n}$  is defined as:

$$A_{m,n} = \int_S p_n d\vec{A} \cdot \vec{\delta}_m \quad (5)$$

where  $p_n$  is the unsteady pressure due to blade vibration in the  $n^{th}$  mode and  $\vec{\delta}_m$  is the  $m^{th}$  modal deflection. The viscous terms are included in the generalized force calculation, along with the pressure term. However, the viscous contributions are not presented here for simplicity. The generalized force can be used to determine the flutter stability of the blade. For an analysis with just one mode, the blade will flutter if the generalized force  $A_{n,n}$  for that mode leads the motion. This provides a simple check of the work-per-cycle calculation.

## SAMPLE RESULTS

In this section, some sample results are presented. The configuration selected is derived from the Energy Efficient Engine (E-cubed) fan rotor. The E-cubed program was established by GE Aircraft Engines under NASA sponsorship in the 1980's to demonstrate component technologies necessary to achieve higher efficiencies and reduce environmental effects in future subsonic turbofan engines. A summary of the program has been presented recently [Smith, 1993]. Details regarding design and performance tests have also been presented [Sullivan and Hager, 1983].

The results presented here are meant to demonstrate the state of development of the code. The fan rotor has 32 blades with a tip diameter of 210.8 cm (83 inches). The inlet flow (axial) Mach number used in this calculation is 0.5. The CFD grid is a simple grid with 15 points on the blade surface in both the chordwise and spanwise

directions. It is assumed that the tip gap is zero. The finite-element structural dynamics data is for a grid with 224 points. The results presented are for an inviscid run of the code. The code has been run in the viscous mode for other configurations.

To begin, a steady solution is obtained for this configuration. The aeroelastic calculations are then performed. Figure 1 shows the finite-element and CFD grids on the blade surface. It is to be noted that the blade planforms from the two grids are slightly different. In the regions where the two planforms do not match, extrapolation (rather than interpolation) is used to transfer the modal deflections from the finite-element grid to the CFD grid, and hence there is potential for errors at these locations

Figure 2 shows the original and interpolated modal deflections corresponding to the first mode. The quantity plotted is the magnitude of the deflection at each grid point. Note that the original data on the finite-element grid is provided on a mean surface, whereas the interpolated data is for the CFD grid on the two distinct blade surfaces. Overall, the interpolated deflections match the original deflections. However, some differences are noted in the blade tip region. Referring to Figure 1, it can be noted that this is one of the areas in which the blade planforms from the CFD grid and the finite-element grid do not match. Figure 3 shows the original and interpolated modal deflections for the second mode. In this case, no significant disagreement can be seen between the original and interpolated data.

Aeroelastic calculations have been performed for the first two modes separately. These two modes have natural frequencies of about 72 Hz and 164 Hz respectively. Aeroelastic calculations were performed for these modes at their natural vibration frequencies, using 100 computational time steps per cycle of blade vibration. Note that, the time step used in the two calculations is not the same. In Figure 4, the instantaneous work is plotted against the time for blade vibration in the first mode. The amplitude of blade vibration used in this calculation results in a maximum deflection of the blade of about 0.9% of the blade tip diameter. The code was run for eight cycles of blade vibration. The variation of instantaneous work with time shows that the flow has become periodic in time. The variation is seen to be nearly sinusoidal, indicating the absence of significant non-linear effects (as evidenced by the absence of higher harmonic content). This may be attributed to the subsonic flowfield. Also, the results indicate that the selected amplitude of blade vibration does not result in any non-linear effects.

In Figure 5, the variation of the cumulative work, from the beginning of the current vibration cycle, is plotted. This quantity starts at zero at the beginning of each

vibration cycle of the blade. At the end of the cycle, the cumulative work done is the work-per-cycle. This is represented as a symbol at the end of each cycle of vibration. After eight cycles, it can be seen that the work-per-cycle remains negative. Thus, work is being done by the blade, and this shows that the blade is stable under the conditions of the analysis.

Figure 6 shows the work-per-cycle after each cycle of vibration. This information is also seen in Figure 5, although on a slightly different scale. It is presented to show the convergence of the flow to periodicity in time. For the configuration analyzed, it can be seen that the work-per-cycle does not vary much after the fourth cycle of blade vibration.

Figure 7 shows the variation of the generalized force on the blade ( $A_{11}$ ). The motion of the blade, given by Equation (2), is also shown. It may be seen that the generalized force  $A_{11}$  lags the motion. For an analysis with just one mode, this indicates that the blade vibrations are stable, since a force lagging the motion will not result in work being done on the blade. This is a verification of the conclusion reached from the work-per-cycle calculation.

Finally, results are presented for the blade vibrating in the second mode. Calculations are performed for an amplitude of blade vibration that results in a maximum deflection of the blade of about 0.2% blade tip diameter. Figure 8 shows the instantaneous work plotted against the time. Although the instantaneous work becomes periodic in time after about four or five cycles, the variation is seen to be significantly non-linear (as evidenced by the higher harmonic content). This is in contrast to the nearly linear variation obtained for the first mode (Figure 4) for a comparatively larger maximum blade deflection. The cause of this non-linear behavior is unknown and is being investigated. The response is expected to be linear for a sufficiently small amplitude. This is seen in Figure 9, where the amplitude of vibration is reduced in half (0.1% blade tip diameter). It should be noted that the work-per-cycle approach is valid for either amplitude, since the approach only requires a periodic response, not necessarily a linear one.

Figure 10 shows the work-per-cycle for blade vibration in the second mode for the smaller amplitude. It can be seen that the work-per-cycle converges to a small negative value. Note that the work-per-cycle is not normalized by the amplitude of vibration. Hence, the smaller values work-per-cycle are partly a result of the smaller amplitude. The calculation indicates that the blade vibrations in the second mode are stable. It should be noted that the work-per-cycle continues to change slightly, even after eight cycles of blade vibration.

## CONCLUDING REMARKS

An aeroelastic analysis code named TURBO-AE has been developed. The starting point for the development was an Euler / Navier-Stokes unsteady aerodynamic code named TURBO. Routines have been developed to interpolate the structural deflections from the finite-element grid to the CFD grid. Grid deformation routines have been developed to calculate a new grid for the deformed blade at each time step. Routines have been developed for the calculation of work and generalized forces. These routines have been verified by running the code for a realistic configuration.

Results have been presented to show the working of the code for two modes of blade vibration. Dynamically, the blade is seen to be stable in both the first and second modes. The results for the first mode show that the force acting on the blade is linear at the selected amplitude of vibration. The results for the second mode show that a non-linear response is obtained for a fairly small amplitude of vibration. However, a reduction of amplitude results in a linear response, as expected.

The calculations for the second mode illustrate an advantage of the work-per-cycle approach, namely, it remains valid even if the force is non-linear. However, the work-per-cycle approach suffers from an assumption that the aerodynamics and the structural dynamics can be decoupled.

A major limitation of the code is that it is currently restricted to the analysis of in-phase blade motions. In a propulsion component, fan, compressor, or turbine, it is necessary to consider the various interblade phase angles at which flutter can occur. Hence, in the future, the code will be extended to allow the analysis of arbitrary interblade phase angles. This can be accomplished either by including multiple blade passages in the calculations, or by using a single blade passage with time (or phase) shifted boundary conditions. Also, it is necessary that the TURBO-AE code be exercised to evaluate its ability to analyze and predict flutter for conditions in which viscous effects are significant. This is also planned for the future.

## ACKNOWLEDGEMENTS

The *TURBO* code was developed by a team of researchers which included David L. Whitfield, J. Mark Janus, Jen-Ping Chen, and Timothy W. Swafford, all at Mississippi State University. The development of the *TURBO* code was supported and guided by John F. Groeneweg and Dennis L. Huff of the Propeller and Acoustics

Technology Branch, by Lawrence J. Bober and Kestutis C. Civinskas of the Turbomachinery Technology Branch, and by Anthony J. Strazisar and Eric R. McFarland of the Turbomachinery Flow Physics Branch, all at the NASA Lewis Research Center. The development of the aeroelastic *TURBO-AE* code is also being supported by the above individuals, and by Peter G. Batterton and John E. Rohde of the Advanced Subsonic Technology (AST) Project Office at NASA Lewis Research Center. The authors would like to gratefully acknowledge the support provided. This work would not have been possible without this support. The authors would also like to thank John J. Adamczyk of the Lewis Research Academy, NASA Lewis Research Center for his helpful suggestions and guidance.

## REFERENCES

Bakhle, M. A., and Reddy, T. S. R., 1993, "Unsteady Aerodynamics and Flutter of Propfans Using a Three-Dimensional Full-Potential Solver", AIAA Paper AIAA-93-1633.

Bakhle, M. A. et al., 1993, "Unsteady Aerodynamics and Flutter Based on the Potential Equation", AIAA Paper AIAA-93-2086.

Carstens, V., 1994, "Computation of Unsteady Transonic 3D-Flow in Oscillating Turbomachinery Bladings by an Euler Algorithm with Deforming Grids", Proceedings of the 7th International Symposium on Unsteady Aerodynamics and Aeroelasticity of Turbomachines, Fukuoka, Japan, September 25-29.

Chen, J. P., 1991, "Unsteady Three-Dimensional Thin-Layer Navier-Stokes Solutions for Turbomachinery in Transonic Flow", Ph.D. Dissertation, Mississippi State University, Mississippi.

Gerolymos, G. A., and Vallet, I., 1994, "Validation of 3D Euler Methods for Vibrating Cascade Aerodynamics", ASME Paper 94-GT-294.

Hall, K. C., 1992, "Calculation of Three-Dimensional Unsteady Flows in Turbomachinery Using the Linearized Harmonic Euler Equations", AIAA Paper 92-0665.

He, L., and Denton, J. D., 1993, "Three-Dimensional Time-Marching Inviscid and Viscous Solutions for Unsteady Flows Around Vibrating Blades", ASME Paper 93-GT-92.

Huff, D. L., 1989, "Numerical Analysis of Flow Through Oscillating Cascade Sections", AIAA Paper AIAA-89-0437.

Janus, J. M., 1989, "Advanced 3-D CFD Algorithm for Turbomachinery", Ph.D. Dissertation, Mississippi State University, Mississippi.

Kaza, K. R. V. et al., 1989, "Analytical Flutter Investigation of a Composite Propfan Model", Journal of Aircraft, Vol. 26, No. 8, pp. 772-780.

Peitsch, D., Gallus, H. E., and Weber, S., 1994, "Prediction of Unsteady 2D Flow in Turbomachinery Bladings", Proceedings of the 7th International Symposium on Unsteady Aerodynamics and Aeroelasticity of Turbomachines, Fukuoka, Japan, September 25-29.

Smith, L., 1993, "NASA/GE Fan and Compressor Research Accomplishments", ASME Paper 93-GT-315.

Srivastava, R. and Reddy, T. S. R. , 1995, "Aeroelastic Analysis of Ducted Rotors", presented at the 1995 International Mechanical Engineering Congress and Exposition.

Sullivan, T. J. and Hager, R. D. , 1983, "The Aerodynamic Design and Performance of the General Electric / NASA E-cubed Fan", AIAA Paper AIAA-83-1160.

Williams, M. H., 1990, "An Unsteady Lifting Surface Method for Single Rotation Propellers", NASA CR-4302.

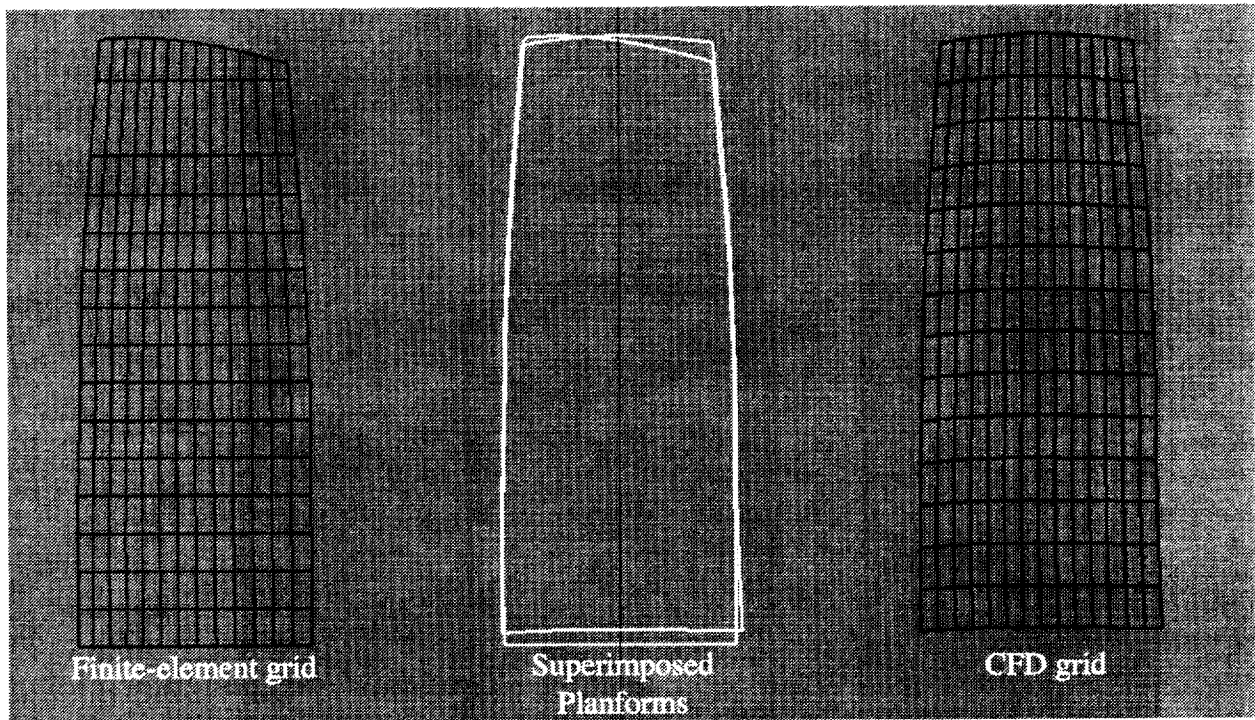


Figure 1: Typical finite-element and CFD grids, and superimposed planforms.

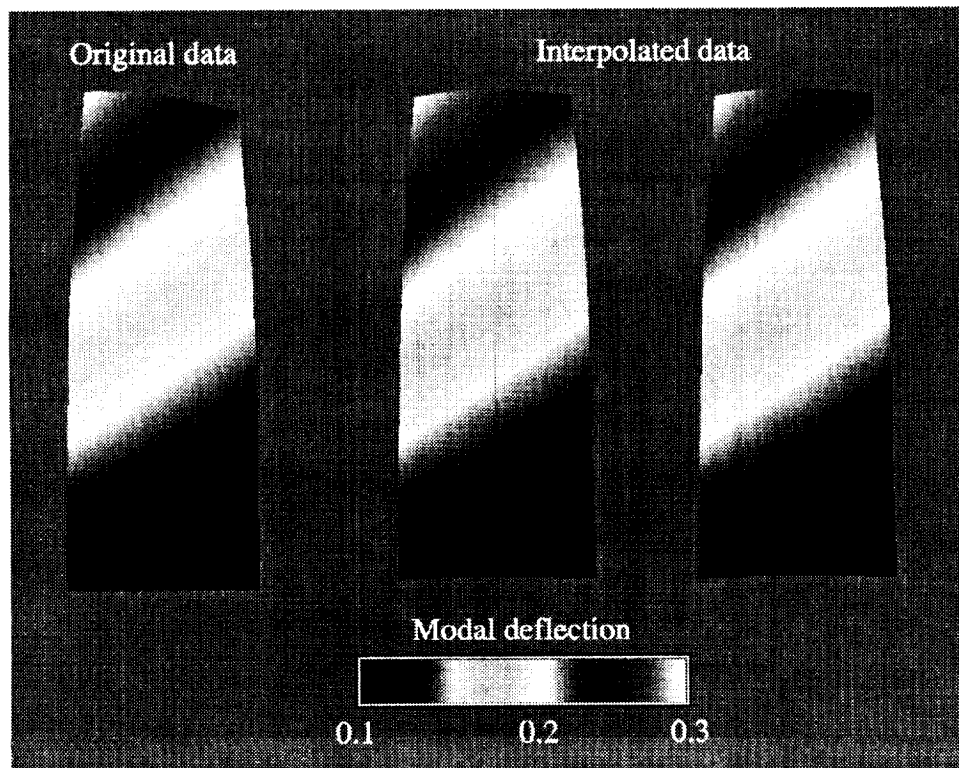


Figure 2: Original and interpolated modal deflections for first mode; interpolated data is for two blade surfaces.

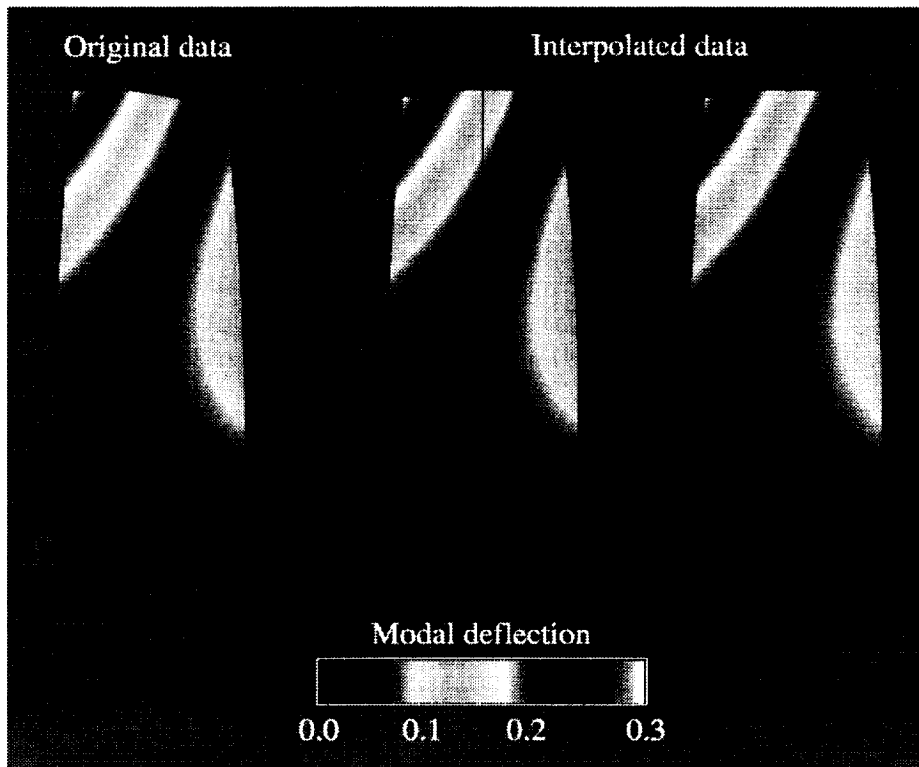


Figure 3: Original and interpolated modal deflections for second mode; interpolated data is for two blade surfaces.

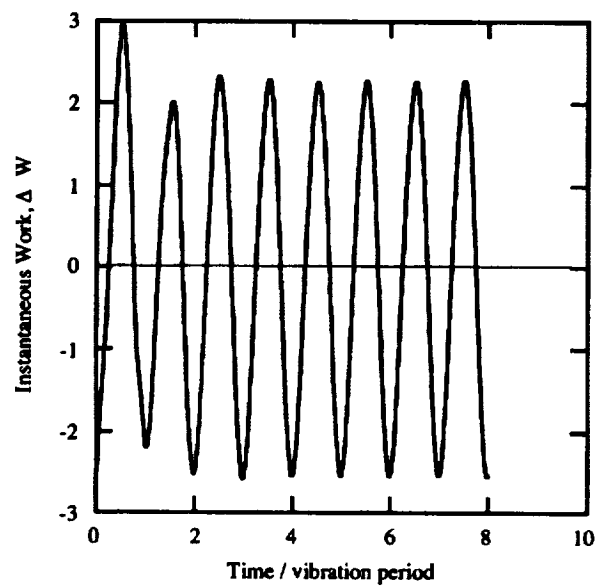


Figure 4: Instantaneous work done on blade vibrating in first mode.



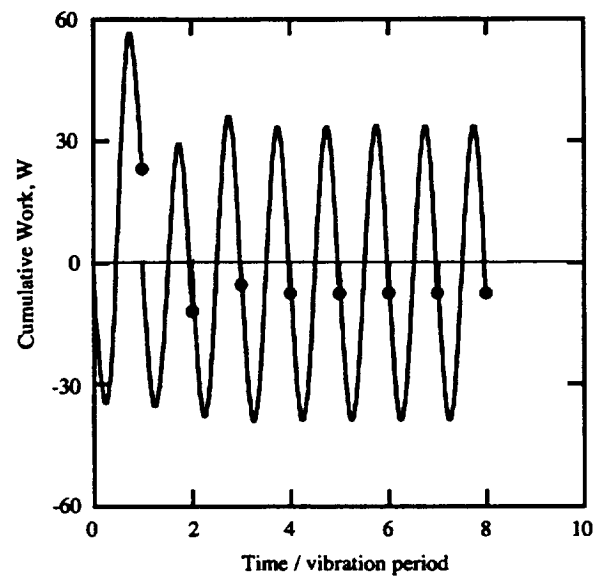


Figure 5: Cumulative work (from beginning of each cycle) done on blade vibrating in first mode. Symbols indicate the value at the end of each cycle.

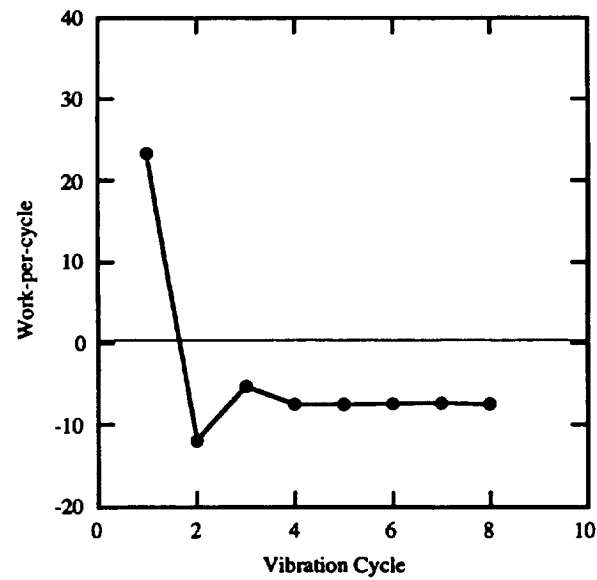


Figure 6: Work-per-cycle for blade vibrating in first mode.

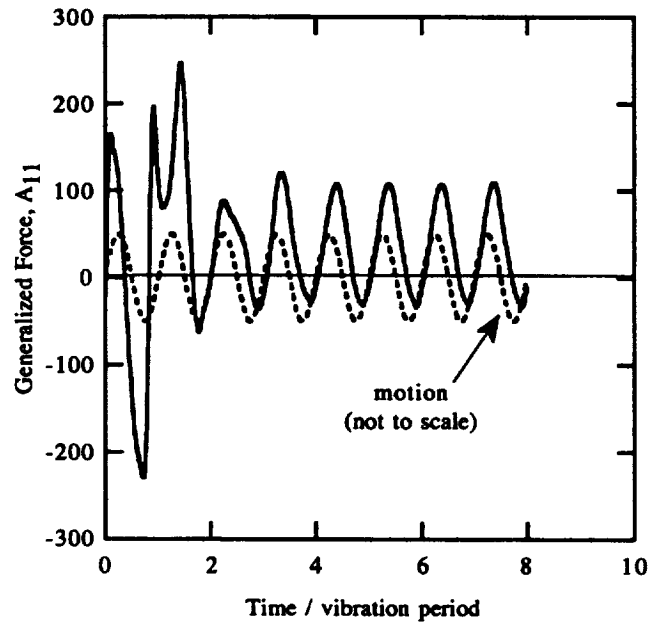


Figure 7: Generalized force acting on blade vibrating in first mode.

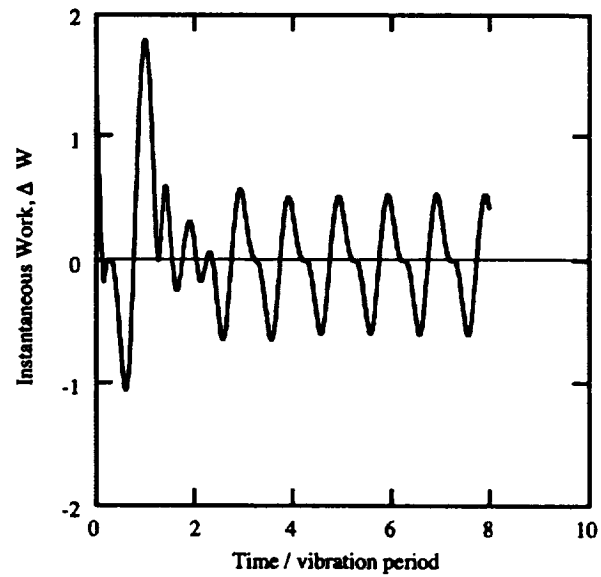


Figure 8: Instantaneous work done on blade vibrating in second mode with maximum blade deflection 0.2% blade tip diameter.

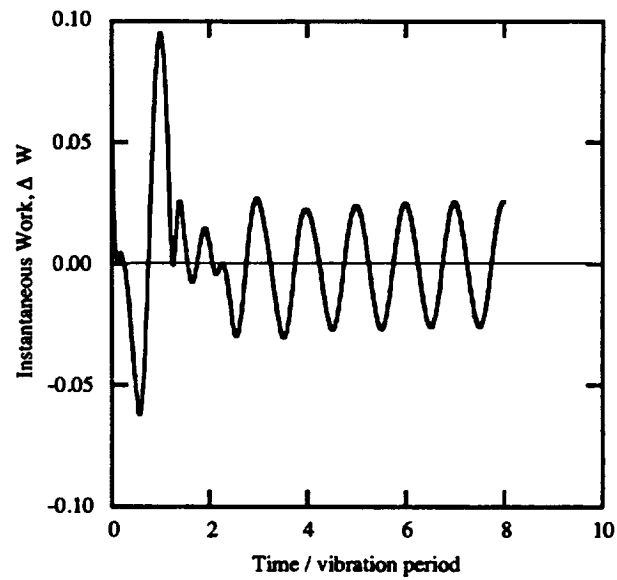


Figure 9: Instantaneous work done on blade vibrating in second mode with maximum blade deflection 0.1% blade tip diameter.

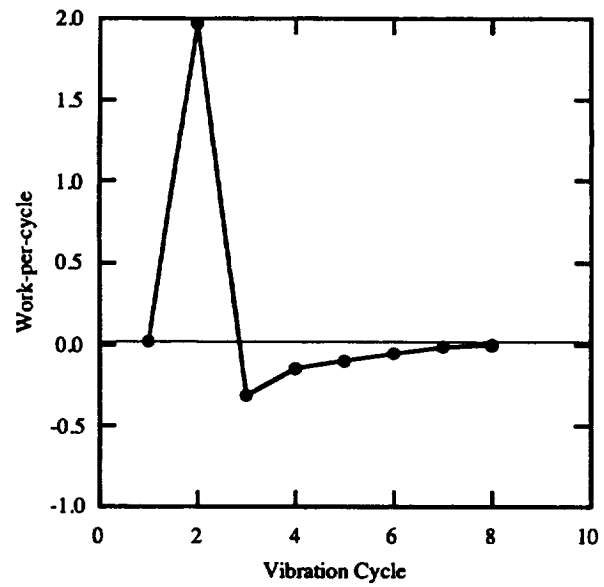


Figure 10: Work-per-cycle for blade vibrating in second mode.

REPORT DOCUMENTATION PAGE			Form Approved OMB No. 0704-0188	
Public reporting burden for this collection of information is estimated to average 1 hour per response, including the time for reviewing instructions, searching existing data sources, gathering and maintaining the data needed, and completing and reviewing the collection of information. Send comments regarding this burden estimate or any other aspect of this collection of information, including suggestions for reducing this burden, to Washington Headquarters Services, Directorate for Information Operations and Reports, 1215 Jefferson Davis Highway, Suite 1204, Arlington, VA 22202-4302, and to the Office of Management and Budget, Paperwork Reduction Project (0704-0188), Washington, DC 20503.				
1. AGENCY USE ONLY (Leave blank)	2. REPORT DATE November 1996	3. REPORT TYPE AND DATES COVERED Technical Memorandum		
4. TITLE AND SUBTITLE Development of an Aeroelastic Code Based on an Euler/Navier-Stokes Aerodynamic Solver		5. FUNDING NUMBERS  WU-538-06-14 NAG3-1803		
6. AUTHOR(S) Milind A. Bakhle, Rakesh Srivastava, Theo G. Keith, Jr, George L. Stefko, and J. Mark Janus				
7. PERFORMING ORGANIZATION NAME(S) AND ADDRESS(ES) National Aeronautics and Space Administration Lewis Research Center Cleveland, Ohio 44135-3191		8. PERFORMING ORGANIZATION REPORT NUMBER  E-10523		
9. SPONSORING/MONITORING AGENCY NAME(S) AND ADDRESS(ES) National Aeronautics and Space Administration Washington, DC 20546-0001		10. SPONSORING/MONITORING AGENCY REPORT NUMBER  NASA TM-107362		
11. SUPPLEMENTARY NOTES Milind A. Bakhle, Rakesh Srivastava, and Theo G. Keith, Jr., University of Toledo, Toledo, Ohio; George L. Stefko, NASA Lewis Research Center, Cleveland, Ohio; J. Mark Janus, Mississippi State University, Mississippi State, Mississippi. Responsible person, George L. Stefko, organization code 5230, (216) 433-3920.				
12a. DISTRIBUTION/AVAILABILITY STATEMENT  Unclassified - Unlimited Subject Category 39  This publication is available from the NASA Center for AeroSpace Information, (301) 621-0390.		12b. DISTRIBUTION CODE		
13. ABSTRACT (Maximum 200 words)  This paper describes the development of an aeroelastic code (TURBO-AE) based on an Euler/Navier-Stokes unsteady aerodynamic analysis. A brief review of the relevant research in the area of propulsion aeroelasticity is presented. The paper briefly describes the original Euler/Navier-Stokes code (TURBO) and then details the development of the aeroelastic extensions. The aeroelastic formulation is described. The modeling of the dynamics of the blade using a modal approach is detailed, along with the grid deformation approach used to model the elastic deformation of the blade. The work-per-cycle approach used to evaluate aeroelastic stability is described. Representative results used to verify the code are presented. The paper concludes with an evaluation of the development thus far, and some plans for further development and validation of the TURBO-AE code.				
14. SUBJECT TERMS Aeroelasticity; Flutter; Viscous; Inviscid; Navier-Stokes			15. NUMBER OF PAGES 19	
			16. PRICE CODE A03	
17. SECURITY CLASSIFICATION OF REPORT Unclassified	18. SECURITY CLASSIFICATION OF THIS PAGE Unclassified	19. SECURITY CLASSIFICATION OF ABSTRACT Unclassified	20. LIMITATION OF ABSTRACT	